

# FLAMMABILITY LIMITS AND LAMINAR FLAME SPEED OF HYDROGEN-AIR MIXTURES AT SUB-ATMOSPHERIC PRESSURES

M. Kuznetsov\*<sup>1</sup>, S. Kobelt<sup>1</sup>, J. Grune<sup>2</sup>, T. Jordan<sup>1</sup>

<sup>1</sup> Pro-Science GmbH, Germany

<sup>2</sup> Institute for Energy and Nuclear Energy, Karlsruhe Institute of Technology, Germany

\*Corresponding author: [kuznetsov@kit.edu](mailto:kuznetsov@kit.edu)

## ABSTRACT

Hydrogen behavior at elevated pressures and temperatures was intensively investigated by numerous investigators. Nevertheless, there is a lack of experimental data on hydrogen ignition and combustion at reduced sub-atmospheric pressures. Such conditions are related to the facilities operating under vacuum or sub-atmospheric conditions, for instance like ITER vacuum vessel. Main goal of current work was an experimental evaluation of such fundamental properties of hydrogen-air mixtures as flammability limits and laminar flame speed at sub-atmospheric pressures. A spherical explosion chamber with a volume of 8.2 dm<sup>3</sup> was used in the experiments. A pressure method and high-speed camera combined with schlieren system for flame visualization were used in this work. Upper and lower flammability limits and laminar flame velocity have been experimentally evaluated in the range of 4-80% hydrogen in air at initial pressures 25-1000 mbar. An extraction of basic flame properties as Markstein length, overall reaction order and activation energy was done from experimental data on laminar burning velocity.

## 1.0 INTRODUCTION

The necessary strategies for the safe handling of hydrogen are developed by the research group "Hydrogen" of the Institute for Nuclear and Energy Technologies (IKET) of the Karlsruhe Institute of Technology (KIT). The focus of the research are, for example, safety strategies against hydrogen accidents in nuclear reactors and as well as hydrogen and dust explosions in the planned fusion reactor ITER. The normal operating pressure of the ITER vacuum vessel (VV) is sub-atmospheric. The water leakage and followed by interaction with hot beryllium dust in the VV after an air ingress from ambient atmosphere may lead to the formation of combustible hydrogen-air mixture [1]. This was the reason why accident scenarios at the ITER operating conditions such as loss of vacuum (LOVA) accident consider formation of hydrogen-air mixtures at sub-atmospheric pressures [1-3]. Additionally, there are vacuum furnaces, where a hydrogen atmosphere is used for the heating treatment at sub-atmospheric pressures [4]. The flammability properties of such mixtures are well-known at atmospheric and elevated pressures as well [5-8]. Only one paper [4] is related to the flammability of hydrogen-air mixtures at sub-atmospheric pressures and ambient temperature. The lowest ignition pressure of 150 mbar was achieved in this work for the high energy spark and hot wire ignition of a hydrogen-air mixture (30% H<sub>2</sub>). The Upper and Lower Flammability Limits (UFL and LFL) of hydrogen-air mixtures at sub-atmospheric pressures have not been investigated in details.

The laminar burning velocity  $S_L$  is an important overall characteristic of the reactivity of combustible mixtures. It is used as a measure of the combustion rate in numerical models to predict the dynamics of combustion. Laminar burning velocity measurements can be used to evaluate the laminar flame thickness  $\delta$ , the overall activation energy  $E_a$ , and the reaction order  $n$  for the dimensionless analysis of a turbulent combustion with respect to estimate the flame stability and flame acceleration potential. The overall reaction order  $n$  and energy activation indicate correspondingly the pressure and temperature influence on the combustion rate. Only few works [9-11] have investigated an effect of reduced pressure on burning rate and such flame properties as reaction order, Markstein number and flame/stretch interaction and flame stability at sub-atmospheric pressures up to 0.2 bar.

## 2.0 EXPERIMENTAL PROCEDURE

Experiments on the flammability limits at sub-atmospheric pressures were performed in a spherical stainless steel explosion bomb of 25 cm internal diameter and an inner volume of  $V = 8.2 \text{ dm}^3$  (Fig. 1). The bomb has two quartz windows for optical observations and several ports for pressure gauges (PCB 112A and PCB 113A) and thermocouples to record pressure and temperature of the combustion process. The shape and size of the bomb were chosen in accordance with the German Standard pNEN1839(B) for the flammability tests. An induction spark plug and a hot wire were used to ignite the test mixtures. The maximum ignition energy in the experiments was about 12.5 J.

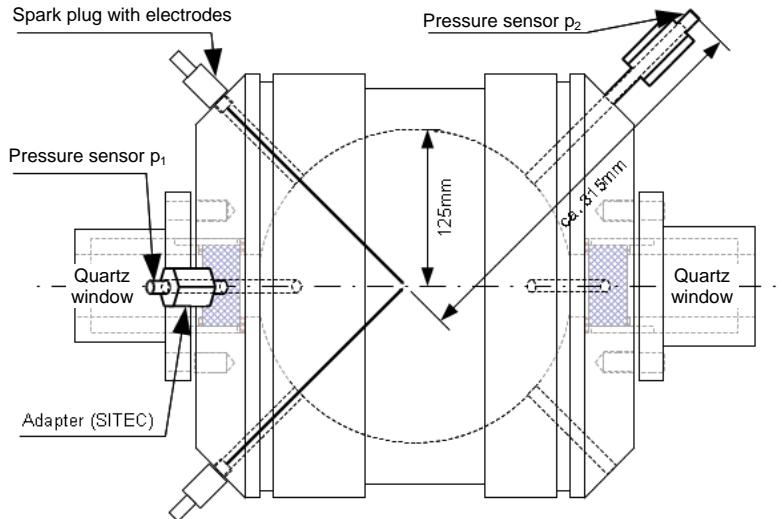


Figure 1. Schematic of explosion chamber

The experimental procedure for evaluation of the flammability limits consisted of pressure measurements combined with a visual observation of the tested mixture after the ignition. A pressure signal of 10 times higher than the signal from the ignition source itself was used as a flammability criterion. This means that for the constant volume an energy release due to ignition and combustion processes is more than 10 times higher than from an ignition device itself. Another evidence of the ignition phenomena was proven using a high speed camera with a frame rate up to 250000 frames/sec. Figure 2 shows a sequence of high speed photo of the ignition process near the flammability limit. Because of too low flame speed an effect of buoyancy is dominating and the flame develops preferably to the top. Finally, the combustion process occupies whole volume. In the case of “no ignition” the mixture might locally be ignited but the flame did not propagate into the volume. It quenches within a short time at the small distance from an igniter.

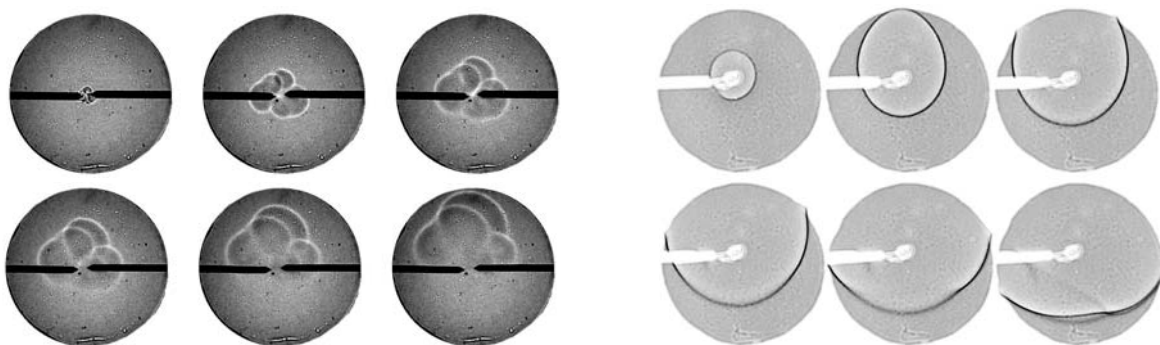


Figure 2. High speed photos of ignition process near lower ( $5\% \text{H}_2$  – left, time step = 15 ms) and upper ( $76\% \text{H}_2$  –right, time step = 3.6 ms) flammability limits ( $p_0 = 1000 \text{ mbar}$ ).

The experimental setup to measure the laminar flame velocity was the same as for the flammability limits (Fig. 1). Evaluations of the laminar burning velocities were made using a high speed cinematography combined with a schlieren system and using a standard spherical bomb method based on pressure measurements. The propagation speed of a real flame front relative to the unburned gas mixture may differ from the theoretical laminar flame speed  $S_L$ . This is primarily due to the wrinkling of flame front and its local stretching. At the initial stage of flame propagation according to paper [12] the effect of flame stretch rate  $K$  on laminar flame velocity was taken into account as follows

$$S_L = S_{L,s} - L_M \cdot K, \quad (1)$$

$$K = \frac{1}{A} \frac{dA}{dt} = \frac{2}{r_b} \frac{dr_b}{dt} \quad (\text{for spherical flame}), \quad (2)$$

where  $A$  is the flame area;  $S_L = dr_b/dt$  (3) is the stretched flame speed;  $r_b$  is the instantaneous flame radius directly measured from the schlieren images of a flame or calculated using initial part of pressure records;  $L_M$  is the Markstein length. A positive Markstein length indicates the flame is stable to the diffusional-thermal effect, whereas a negative Markstein length indicates the flame surface will be distorted due to diffusional-thermal instability leading to the acceleration of flame speed and the formation of a cellular structure. The flame radius  $r_b$  and the stretched flame speed  $S_L$  were also evaluated in current work by Dahoe [13]:

$$\frac{r_b(t)}{R} = \left[ 1 - \left( \frac{p_0}{p} \right)^{1/\gamma} \frac{p_e - p}{p_e - p_0} \right]^{1/3} \quad \text{and} \quad (4)$$

$$S_L(t) = \frac{r_{\text{exp}}}{3} \frac{1}{p_e - p_0} \left( \frac{p_0}{p} \right)^{1/\gamma} \left[ 1 - \left( \frac{p_0}{p} \right)^{1/\gamma} \frac{p_e - p}{p_e - p_0} \right]^{-2/3} \frac{dp}{dt}, \quad (5)$$

where  $p_0$  is the pressure at the initial state;  $p_e$  the theoretical maximum combustion pressure;  $\gamma = C_p/C_v$  is the adiabatic exponent;  $R$  is the inner radius of spherical bomb. Current values of pressure  $p$  and its derivative  $dp/dt$  can be taken from experimental pressure-time histories. In order to eliminate an effect of combustion pressure and adiabatic compression temperature only initial part of the pressure records was used for the flame radius and laminar burning velocity evaluation.

### 3.0 EXPERIMENTAL RESULTS AND DISCUSSION

#### 3.1 Flammability limits

The flammability experiments with H<sub>2</sub>-air mixtures at an initial pressure from 25 mbar to 1000 mbar have been performed within the entire range of flammability 4-80% of hydrogen in air. An overview of all the tests is shown in Fig. 3. Every experimental point indicates “ignition” or “no ignition” event. For all ignitions of H<sub>2</sub>-air mixtures the pressure-time history and the schlieren images were evaluated to determine the combustion regime and the laminar flame speed. Additionally the maximum combustion pressure of combustion was evaluated. As it follows from Fig. 3, the data obtained in the present work are quite consistent with the data of the referred work [4] with the difference that the minimum ignition pressure in our experiments was 100 mbar for spark ignition and below 50 mbar for hot wire ignition, compared to 150 mbar in paper [4]. The Lower Flammability Limit (LFL) is not sensitive to the initial pressure. It remains at about 4% hydrogen in air as it is at atmospheric pressure, independent of the initial pressure. The Upper Flammability Limit was found to be quite sensitive to the initial pressure in the range of 50-1000 mbar. The UFL extends from 75%H<sub>2</sub> at 1000 mbar to 80%H<sub>2</sub> at pressures in the range of 200-500 mbar, and then below 200 mbar it reduces from 80%H<sub>2</sub> to 50%H<sub>2</sub> at a pressure of 50 mbar.

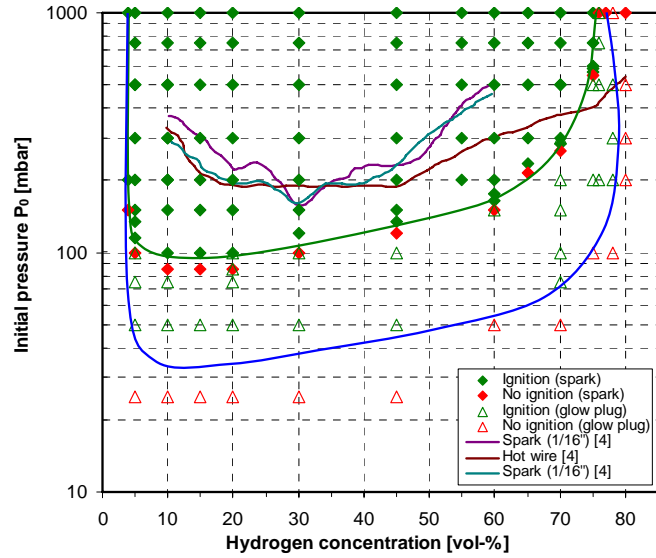


Figure 3. Flammability limits of hydrogen-air mixtures at sub-atmospheric pressures ( $T = 293 \text{ K}$ )

### 3.2 Combustion pressure

Dynamic pressure-time history during the combustion process allows to make qualitative statements about the combustion process and to determine the laminar flame speed. Of particular interest is the influence of initial pressure and concentration of fuel on the combustion process. For all investigated combustible mixture a progressive increase of internal pressure (Fig. 4) inside the bomb develops after the ignition process starts after a certain period of time. This is caused by the release of energy of the strongly exothermic combustion reaction. The slope  $dp/dt$  increased continuously during combustion process and reached its maximum at the end of the turning point of the pressure-time curve. The maximum combustion pressure is an integral characteristic of combustion process. For all tested hydrogen-air mixtures the maximum pressure resulting from the combustion process increases with increasing initial pressure with the relationship between maximum combustion pressure and initial pressure as  $p_{\max}/p_0$ , which is nearly constant for a certain hydrogen concentration. This is obviously because the combustion energy is proportional to the density of reactants.

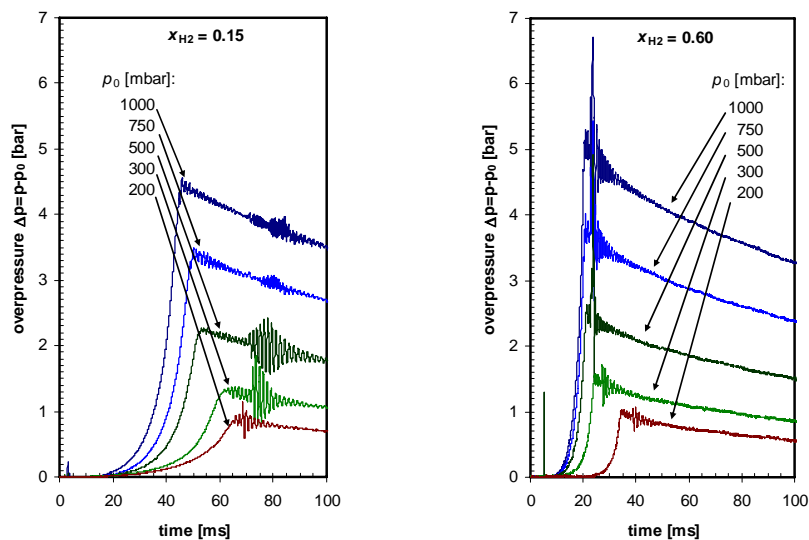


Figure 4. Typical pressure-time history for lean (15% $\text{H}_2$ ) and rich (60% $\text{H}_2$ ) hydrogen-air mixtures at different initial pressures.

Figure 5 shows dependence of maximum combustion pressure against hydrogen concentration at different initial pressure. The highest maximum pressure for stoichiometric mixture has been achieved because the consumption degree of fuel and oxidizer is the greatest. The lowest pressure occurred near the lean or rich flammability limit. Good consistency of combustion pressure  $p_{\max}$  and theoretical adiabatic complete combustion pressure  $P_{\text{icc}}$  is seen in Fig. 5. For the most cases, the measured combustion pressure is lower than the theoretical, that may be due to heat losses and incipient condensation processes towards the end of the combustion [14]. For the stoichiometric mixtures, the maximum pressure difference tends to be larger with increasing pressure. A reason for this could be because of oscillations of the experimental pressure-time history. This makes difficult a precise evaluation of final combustion pressure. For concentrations near the flammability limits greater differences between measured and calculated combustion pressures are observed. Because the explosion duration for very lean and rich mixtures strongly increases, the pressure losses by heat transfer and steam condensation increase. Another reason for maximum pressure difference could be incompleteness of combustion due to flame instabilities.

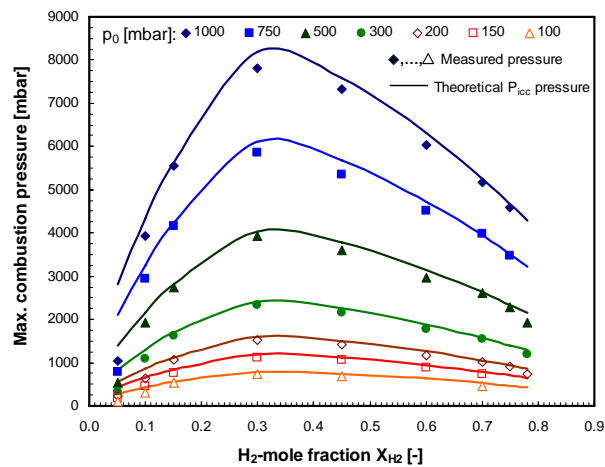


Figure 5. Measured and theoretical maximum combustion pressures in relation to the  $\text{H}_2$  concentrations for different initial pressure  $p_0$

### 3.3 Results of schlieren method

In addition to the measurements of internal pressure, a high speed schlieren imaging method was used in this work on the one hand to visualize the history of combustion and on the other hand to determine the propagation velocity of the flame front in an early phase of combustion. This is the advantage of shadow images procedure concerning the pressure measurement, that the combustion process can be directly analyzed immediately after ignition. Also the visualization of the flame allows to study structure of the flame and its stability or instability. Figure 6 show the sequence of schlieren images of a deflagration in spherical explosion bomb for a lean and a rich mixture at an initial pressure of 1000 mbar. With the exception of the tests near the flammability limits, the flame develops practically as a sphere. A time dependence of the flame radius in two perpendicular directions was used for laminar burning velocity evaluations.

As it was shown later, the effect of electrodes had no significant effect on the values of the laminar flame speed. Nevertheless, the first cracks leading to cellular flame came from the places where the flame contacts with the electrodes. The time of the creation of cell structures depends on the initial pressure as well as the hydrogen concentrations. Generally, it was found that the formation of the cells was increasingly delayed with decreasing initial pressure and increasing fuel content. For example, for a reaction mixture with  $x_{\text{H}_2} = 0.15$  at 1000 mbar the cell formation began immediately after ignition, and the number of cells with progression of combustion is greatly increased (see Fig. 6, left). However, the first cells for the same mixture at an initial pressure of 200 mbar encountered only after

about  $\frac{3}{4}$  of the duration of the explosion. Similarly to the low pressure tests, for a fuel-rich mixture  $x_{H_2} = 0.6$  at 1000 mbar the cellular flame formation appeared only towards the end of the combustion (see Fig. 6, right). For the rich mixtures at reduced initial pressures lower than 300 mbar no cell structure during full reaction time was visible at all.

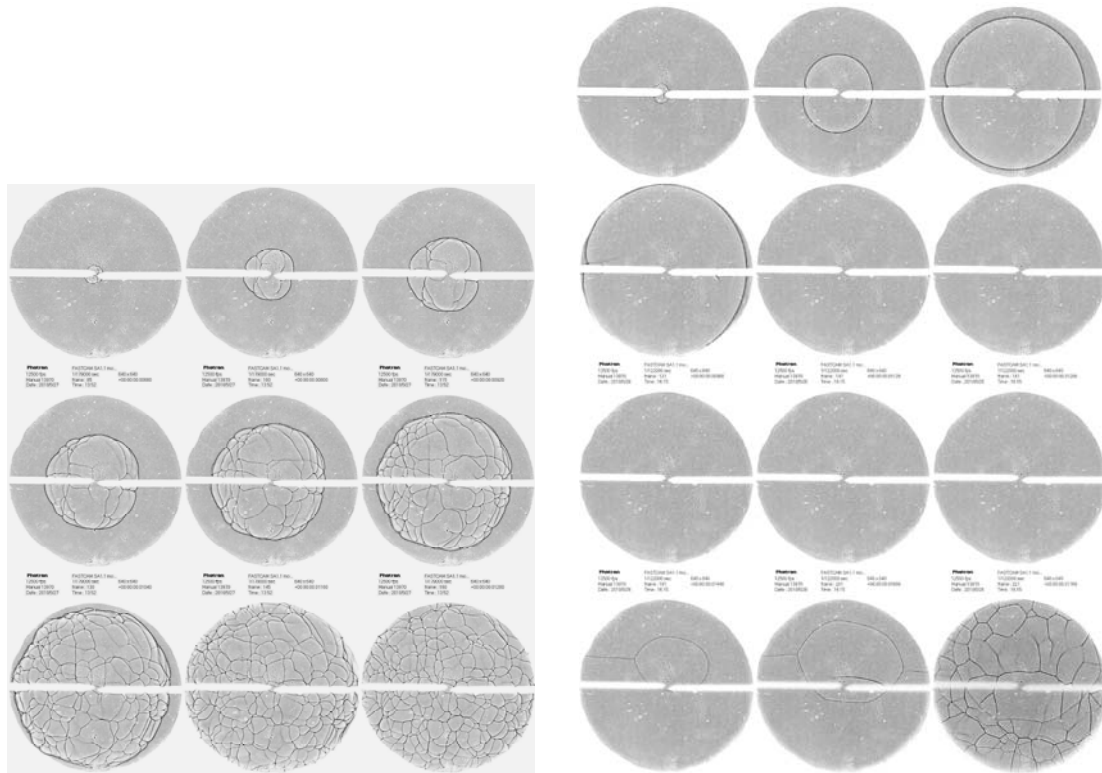


Figure 6. Schlieren images of combustion process for lean (left: 15% $H_2$ , time step = 1.2 ms) and rich (right: 60% $H_2$ , time step = 1.2 ms)  $H_2$ -air mixtures:  $p_0 = 1000$  mbar.

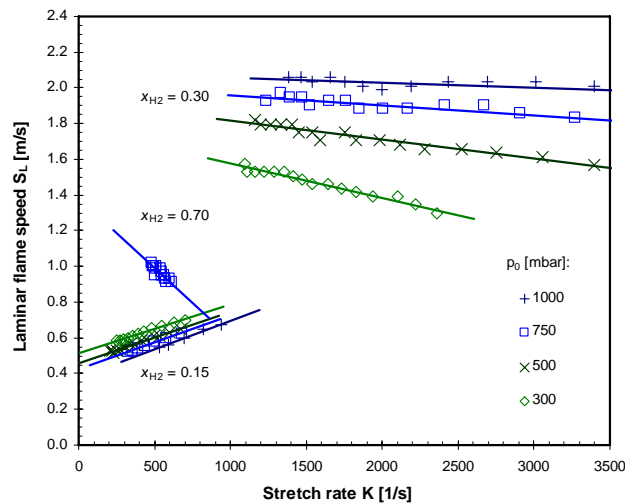


Figure 7. Stretched laminar flame speeds against the flame front stretch rate for different  $H_2$ - air mixtures and different initial pressure. Results of the evaluation of the schlieren images.

Data processing of high speed schlieren images (Fig. 6) allows to evaluate actual flame radius  $r_b$ , stretched flame velocity  $S_L$ , and stretch rate  $K$  according to Eq. (1)-(3). Figure 7 shows the stretched flame propagation speed as a function of stretch rate at different initial pressures and hydrogen mole



fractions. As follows from Eq. (2), the slope of the linear fit for  $S_L - K$  dependence gives a value of Markstein length  $L_M$  as well as the extrapolation of the linear fit  $S_L - K$  to the value  $K = 0$  corresponding to a planar flame gives so called unstretched laminar flame velocity  $S_{L,s}$ . As shown in Fig. 7, that the value of the unstretched laminar flame speed as well as the influence of the flame speed on flame curvature or stretch of the flame depends on a hydrogen mole fraction and an initial pressure.

The relationship between flame speed and fuel concentration the laminar free of stretch flame speed of  $H_2$ -air mixtures is shown in Fig. 8. The smallest burning speeds were measured for very lean mixtures. With increasing concentration of fuel the flame speed increases and reaches its maximum at hydrogen mole fraction of 0.4-0.45. The highest burning rate of  $S_{L,s} = 2.88$  m/s was measured for a hydrogen-air mixture of  $x_{H_2} = 0.4$  (equivalence ratio  $\Phi = 1.6$ ) at an initial pressure of 1000 mbar. Then the laminar flame velocity decreases again with hydrogen concentration increase up to the upper flammability limit. Generally, higher flame speeds were measured for rich mixtures than for lean because of higher thermo conductivity of rich mixtures. Furthermore, it is necessary to note that the laminar flame speed for most of the tested mixtures increases with increasing initial pressure. Only for very lean mixtures ( $x_{H_2} < 0.25$ ,  $\Phi < 0.79$ ) this behavior is opposite. Here, the flame speed slightly increases with decreasing initial pressure (see Fig. 8-9). Effect of the initial pressure is more pronounced in Fig. 8 (right). One can see suppressing effect of the initial pressure on the unstretched laminar velocity for the mixtures leaner than  $x_{H_2} = 0.25$ . The biggest uncertainties (max. 20%) occur for very low pressures and fuel-rich mixtures. This is primarily due to the lower number of meaningful measurement points and partly due to the lower intensity of the schlieren signal at low pressures.

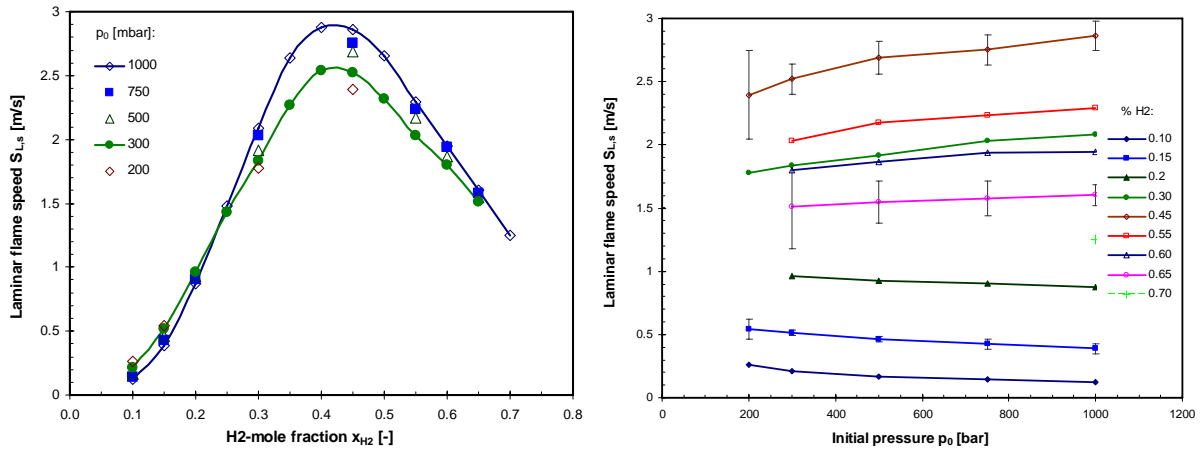


Figure 8. Unstretched laminar flame speeds vs.  $H_2$ -mole fraction (left) and initial pressure (right).  
Results of the evaluation of the schlieren images.

The overall reaction order  $n$  is a parameter responsible for the pressure dependence of laminar velocity. By changing the initial pressure  $p_0$  as shown in Fig. 8 (right) the overall reaction order  $n$  can be obtained. Generally, to evaluate the reaction order  $n$  for a small variation of the initial pressure  $p$  the following equation was used [15]:

$$n = 2 \frac{\partial \ln(S_L)}{\partial \ln(p)} + 2, \quad (6)$$

Figure 9 shows the data of overall reaction order based on the experimental measurements using a schlieren method. Basically the reaction order  $n > 2$ . Only for lean mixtures with  $x_{H_2} < 0.25$  ( $\Phi < 0.79$ ) the reaction order  $n < 2$ . This is in agreement with changing of the pressure dependence of laminar speed at an initial pressure  $x_{H_2} = 0.25$  (Fig. 8, left). What does it mean? Eq. (6) follows from Zeldovich-Frank-Kamenetskii theory [12] and simply for practical purposes the pressure dependence

of laminar flame speed can be written  $S_L \sim (p_0)^\beta$ , where  $\beta = \frac{n}{2} - 1$  is the pressure exponent, same as in paper [10]. This means that the pressure exponent is negative and the initial pressure has suppressing effect on the laminar flame speed if reaction order  $n < 2$ . Experimental data on the pressure dependence of laminar flame speed in the paper [10] are in good consistency with our data.

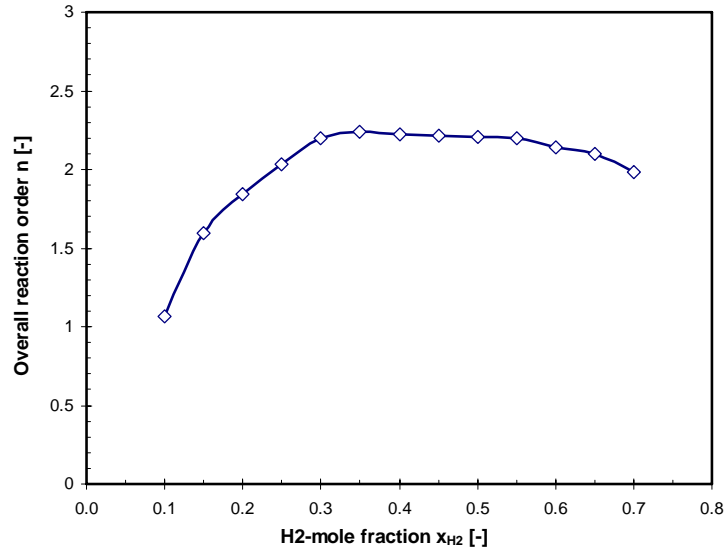


Figure 9. Overall reaction order  $n$  at sub-atmospheric pressures as function of hydrogen mole fraction.

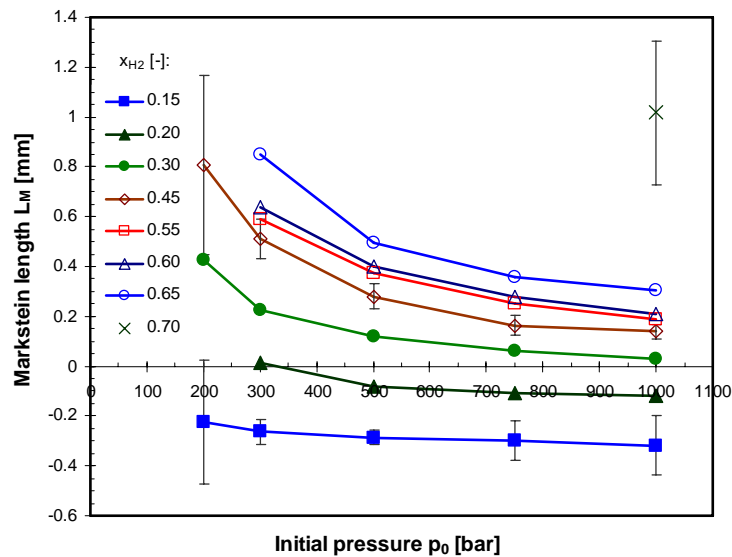


Figure 10. Markstein length depending on the initial pressure for different H<sub>2</sub> concentrations. Results of the evaluation of the schlieren images.

Another effect of the pressure is related to the flame stability, specifically to the influence of flame front stretch on laminar flame speed. According to Eq. (1)-(3) this effect can be specified by Markstein length  $L_M$ . Figure 10 summarizes all data on Markstein length as a function of the initial pressure for different H<sub>2</sub>-air mixtures. As for the laminar flame speed, the largest uncertainties (up to 100%) occur on Markstein length for low pressures and concentrations near the flammability limits.



For all the concentrations, the Markstein length increases progressively with decreasing initial pressure. Also, the concentration of fuel has great influence on the effect of the flame front curvature. Lean mixtures with  $x_{H_2} < 0.25$  ( $\Phi < 0.8$ ) have negative Markstein lengths, while for stoichiometric and rich mixtures positive Markstein lengths were measured. That is that for lean mixtures the stretch effects cause an acceleration of the curved flame front to the planar, while for stoichiometric and rich mixtures they cause a deceleration of the flames (see also Fig. 7).

### 3.4 Comparison of the results with reference data

This section compares the results obtained with the schlieren method in current work with the data of other authors. The results of different works according to the equivalence ratio are plotted in Fig. 11. The data by Kwon et al. [16], Aung et al. [17] and Dowdy et al. [18] were determined on the basis of schlieren photographs and therefore free to stretch. The results of Dahoe [13], Iijima & Takeno [19] and Grumer et al. [20] are based on measurements of the dynamic pressure. For lean and stoichiometric mixtures, all reference values in good agreement with current work. For rich mixtures up to  $x_{H_2} \leq 0.6$  ( $\Phi \leq 3.57$ ) the results by Kwon et al., Dowdy et al., Dahoe and Iijima & Takeno are within the uncertainty of current measurements. Only for very rich mixtures with  $x_{H_2} > 0.6$  the flame speeds in this work are slightly above those of the other authors.

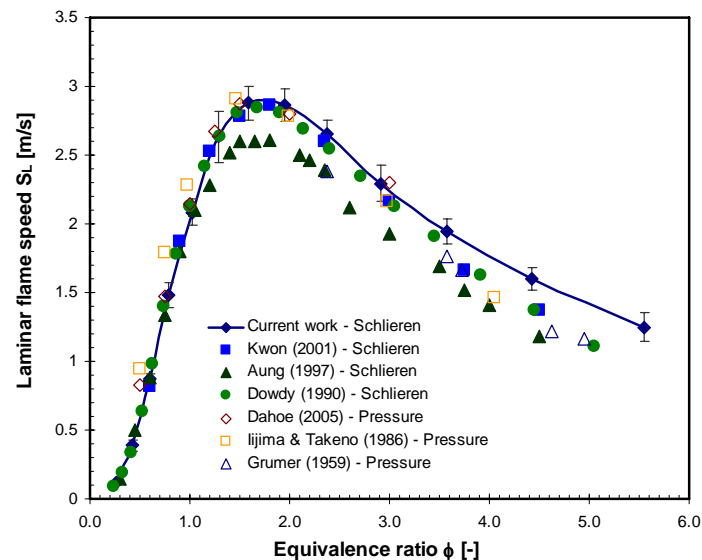


Figure 11. Comparison of the measured laminar flame speed and reference data at  $p_0 = 1.0$  bar.

The reason for such difference for very rich mixtures is unclear. The uncertainty of the measurement of flame speed has no matter because it is smaller than the differences. One of the reasons could be not proper range of the flame radius for the linear approximation because of too small size of optical window. However, the Markstein length for rich mixtures is positive and the value of the unstretched laminar flame speed must be therefore above the window size. In addition, the medium-sized laminar flame speeds given on the basis of the pressure-time history can be corrected if the corresponding Markstein length is known. So corrected results of the pressure method correspond well to the optical values. However with such a correction the values of the other authors for very rich mixtures are still below the values specified in this work. This also may be due to the relatively large uncertainty of the Markstein length of these mixtures.

A similar picture is plotted for reduced pressures and so far only a few works were published. Figure 12 shows a comparison of the unstretched laminar flame speeds in current work with data of Aung et al. [9]. As for 1000 mbar (Fig. 11), current data and the data by Aung [9] for lean and stoichiometric

mixtures at 500 or 300 mbar agreed well. For rich mixtures, the Aung data are considerably lower than in current work.

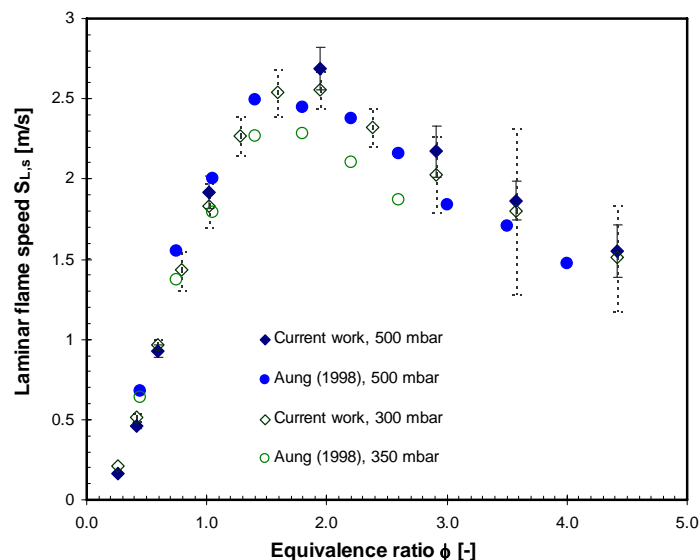


Figure 12. Unstretched laminar flame speeds of H<sub>2</sub>-air mixtures as a function of the equivalence ratio. Initial temperature: 290 - 300 K. Comparison of the measured laminar flame speed and reference data [9] at reduced pressures.

#### 4.0 SUMMARY AND CONCLUSIONS

This work examined the laminar spherical flame propagation for H<sub>2</sub>-air mixtures. The hydrogen content of H<sub>2</sub>-air mixtures was varied between 4 vol.% and 80 vol.%. The initial pressure was between 25 mbar and 1000 mbar. The initial temperature was 285 - 295 K. In addition to an analysis of combustion behavior and the flammability limits of H<sub>2</sub>-air mixtures, the laminar flame speed and the Markstein length of reaction mixtures for a wide range of initial pressures and hydrogen concentration have been evaluated.

The experiments were carried out in an explosion bomb fabricated of stainless steel with a spherical internal volume of 8.2 dm<sup>3</sup>. The bomb had two opposite quartz windows each 50 mm in diameter. The mixture within the flammability limits, which was exploded in the center of the bomb, could propagate as an ideal spherical spread to a bomb radius of 125 mm. A spark plug or a glow plug used for ignition. The laminar flame propagation was analyzed in detail with two methods: the schlieren method and the pressure method. The propagation of the flame by using a schlieren method was visualized in the optical system. This allowed the direct optical observation of the flames and may indicate instability of flame, such as cellular structure. This effect could also be taken into account as the effect of flame front stretch during the calculation of laminar burning rate. In addition, the initial phase of stretch effect was evaluated by pressure method in comparison with the results of the schlieren method.

Upper and lower flammability limits were experimentally evaluated as function of initial pressure in the range 50-1000 mbar. It was found that the lower flammability limit practically does not change up to the pressure 50 mbar. Then the mixture could not be ignited. Very lean mixtures at the LFL with a hydrogen content of 4% vol. could still be ignited, but the flame propagated only upwards and the development of pressure was low. However, very rich mixtures at the UFL with a 78% H<sub>2</sub> seemed to burn almost fully at initial pressures between 200 mbar and 500 mbar. For an initial pressure of 1000 mbar the upper limit of the ignition was at a H<sub>2</sub> concentration of only 76%. Near the flammability

limits there was a significant increase in the ignition energy from 0.005 J up to 7.5 J. No one of the H<sub>2</sub>-air mixtures with current equipment could be ignited at initial pressures less than 25 mbar. Commonly the ignition energy needs to be magnified with decreasing initial pressure.

The laminar unstretched flame speed of H<sub>2</sub>-air mixtures depended on the concentration of fuel as well as on the initial pressure. The smallest burning speeds were measured for very lean mixtures. For H<sub>2</sub> content between 40 mol.% and 45 mol.% the flame speed was found to be maximum. The maximum value measured in this work was 2.88 m/s for 40% H<sub>2</sub> at an initial pressure of 1000 mbar. To characterize pressure dependence of laminar flame speed, the overall reaction order was evaluated for different hydrogen content by changing of the initial pressure. The reaction order less than 2 with a negative pressure dependence was found for lean mixtures with  $x_{\text{H}_2} < 0.25$  ( $\Phi < 0.79$ ). The rest mixtures ( $x_{\text{H}_2} > 0.25$ ) have positive influence of the pressure on laminar flame speed because the reaction order  $n > 2$ .

The effect of the initial pressure can be explained by the influence of the flame front stretch, which can be derived on the basis of the Markstein length. While stoichiometric and rich mixtures had positive Markstein lengths, negative Markstein lengths were measured for lean mixtures. Thus the flame front stretch for lean or rich mixtures resulted in an acceleration or deceleration of the spherical flame with approaching to a planar flame. For all investigated H<sub>2</sub>-air mixtures, the Markstein length increases with decreasing initial pressure. Accordingly, the influence of the flame front stretch for lean or rich mixtures took off with decreasing initial pressure.

Finally, the laminar unstretched flame speeds have been compared with the results of other authors. The good agreement of the data confirm the significance of the presented results. To improve the reliability of the evaluated values, every test should be repeated specifically for rich mixtures at least three times. Still, the feedback of frame rate and resolution of high-speed imaging can be optimized to minimize the uncertainty of individual measurements. If possible, the initial temperature should also remain constant to exclude any influence of the temperature.

Further investigations can be made on the influence of the initial temperature. This is very important in some technical applications, and will therefore have great effect on the respective laminar flame speeds and flammability limits.

## 5.0 ACKNOWLEDGEMENTS

This work was supported by the European Communities under the contract of Association between EURATOM and Forschungszentrum Karlsruhe (currently Karlsruhe Institute of Technology) within the framework of the European Fusion Development Agreement.

## 6.0 REFERENCES

1. Topilski, L., Main parameters and assumptions that should be taken into account in the model of inert gas injection system for hydrogen explosion suppression, ANNEX 2 G 81 TD 29 FE, 2006.
2. Xiao, J., Travis, J.R., Breitung, W., and Jordan, T., Feasibility study of possible prevention of hydrogen combustion in ITER by injection of inert gas, FZK report, EFDA task TW6-TSS-SEA4.5a, 2008.
3. Travis, J.R., Spore, J.W., Royl, P., Lam, K.L., Wilson, T.L., Müller, C., Necker, G.A., Nichols, B.D., Redlinger, R., GASFLOW: a computational fluid dynamics code for gases, aerosols and combustion. Volume 1. Theory and computational model. FZK and LANL Reports, 2001.
4. Jones, T., Explosive nature of hydrogen in partial pressure vacuum, Heat Treating Progress, Jan.–Feb. (2009) 43–46.
5. Kumar, R.K., Flammability limits of hydrogen-oxygen-diluent mixtures. *J. Fire Sci.* 3 (1985) 235–262

6. Schröder, V., Holtappels, K., Explosion characteristics of hydrogen-air and hydrogen-oxygen mixtures at elevated pressures. 2nd International Conference on Hydrogen Safety, 2005.
7. Zabetakis, M.G., Flammability characteristics of combustible gases and vapors, Bulletin 627, US Bureau of Mines, XMBUA, 1965.
8. Kuznetsov, M., Redlinger, R., Flammability limits of hydrogen-air and hydrogen-oxygen mixtures at elevated temperatures. FZK quarter-report, icefuel Project, 2008.
9. Aung, K.T., Hassan, M.I., Faeth, G.M., Effects of Pressure and Nitrogen Dilution on Flame/Stretch Interactions of Laminar Premixed H<sub>2</sub>/O<sub>2</sub>/N<sub>2</sub> Flames. *Comb. Flame* 112 (1998) 1-15.
10. Egolfopoulos, F.N., Law, C.K., An experimental and computational study of the burning rates of ultra-lean to moderately-rich H<sub>2</sub>/O<sub>2</sub>/N<sub>2</sub> laminar flames with pressure variations, Symposium (International) on Combustion, 23 (1991) 333-340.
11. Pareja, J, Burbano, H.J., Amell, A., Carvajal, J., Laminar burning velocities and flame stability analysis of hydrogen/air premixed flames at low pressure, *Int. J. Hydrogen Energy*, 36 (2011) 6317-6324, ISSN 0360-3199
12. Clavin, P., Dynamic behavior of premixed flame fronts in laminar and turbulent flows. *Prog. Energy and. Combust. Sci.* 11 (1985) 1-59
13. Dahoe, A.E., Laminar burning velocities of hydrogen-air mixtures from closed vessel gas explosions. *Journal of Loss Prevention in the Process Industries* 18 (2005) 152-166.
14. Leisenheimer, B, Zum Ausbreitungsverhalten von Deflagrationsfronten in laminaren und turbulenten Brenngas/Luft-Gemischen innerhalb geschlossener Behälter. Dissertation. Universität Karlsruhe (TH) (1997).
15. Sun, C.J., Sung, C.J., He, L., and Law C.K., Dynamics of weakly stretched flames: quantitative description and extraction of global flame parameters, *Comb. Flame* 118 (1999) 108-128.
16. Kwon, O. C., Faeth, G. M., Flame/Stretch Interactions of Premixed Hydrogen-Fueled Flames: Measurements and Predictions. *Combustion and Flame* 124 (2001) 590-610.
17. Aung, K. T., Hassan, M. I., Faeth, G. M., Flame stretch interactions of laminar premixed hydrogen/air flames at normal temperature and pressure. *Combustion and Flame* 109 (1997) 1-24.
18. Dowdy, D. R., Smith, D. B., Taylor, S. C., The use of expanding spherical flames to determine burning velocities and stretch effects in hydrogen/air mixtures. Twenty-Third Symposium (Int.) on Combustion (1990) 325-332.
19. Iijima, T., Takeno, T., Effects of Temperature and Pressure on Burning Velocity. *Combustion and Flame* 65 (1986) 35-43.
20. Grumer, J., Cook, E. B., Kubala, T. A., Considerations Pertaining to Spherical-vessel Combustion. *Combustion and Flame* 3 (1956) 437-446.